

Broadband laser cooling of trapped atoms with ultrafast pulses

B. B. Blinov,* R. N. Kohn, Jr., M. J. Madsen, P. Maunz, D. L. Moehring, and C. Monroe
FOCUS Center and University of Michigan Department of Physics Ann Arbor, MI 48109-1040
 (Dated: May 8, 2019)

We demonstrate broadband laser cooling of atomic ions in an rf trap using ultrafast pulses from a modelocked laser. The temperature of a single ion is measured by observing the size of a time-averaged image of the ion in the known harmonic trap potential. While the lowest observed temperature was only about 1 K, this method efficiently cools very hot atoms and can sufficiently localize trapped atoms to produce near diffraction-limited atomic images.

PACS numbers: 32.80.Pj, 42.50.Vk

Laser cooling of atoms [1, 2] has become a cornerstone of modern day atomic physics. Doppler cooling and its many extensions usually involve narrow-band, continuous-wave lasers that efficiently cool atoms within a narrow velocity range (~ 1 m/s) that corresponds to the radiative linewidth of a typical atomic transition. To increase the velocity capture range, several laser cooling methods were investigated that modulate or effectively broaden a narrow-band laser [3, 4, 5, 6, 7, 8]. Modelocked pulsed lasers have been used to narrow the velocity distribution of atomic beams within several velocity classes given by the bandwidth of each spectral component of the frequency comb [9, 10]. In this letter we report the demonstration of Doppler laser cooling of trapped atoms with individual broadband light pulses from a modelocked laser.

To efficiently capture and cool high-velocity atoms, it is necessary to achieve a laser bandwidth large enough to cover the large range of atomic Doppler shifts. For example, Cd^+ ions used in this experiment are initially created with an average kinetic energy of order 1 eV, which corresponds to an average velocity of about 1300 m/s and a Doppler shift of $\Delta_D \sim 36$ GHz. Power broadening an atomic transition (saturation intensity I_s and natural linewidth γ) would require a laser intensity of $I/I_s \sim (2\Delta_D/\gamma)^2$, which can be prohibitively high. For Cd^+ ($\gamma/2\pi \simeq 50\text{MHz}$, $I_s \simeq 5000\text{W/m}^2$) this requires $I \sim 10^{10}\text{W/m}^2$. Modulating a narrow-band laser to generate high bandwidths would allow for significantly less laser power, but it is technically difficult to generate a 100 GHz wide modulation spectrum [4]. On the other hand, an ultrafast laser whose pulse is a few picoseconds long will naturally have a bandwidth in the above range, as well as sufficient intensity to excite the transition.

The laser cooling rate depends critically on the photon scatter rate, which for a pulsed laser can be no larger than the laser repetition rate R (about 80 MHz for a typical modelocked laser), given that the atom is excited with unit probability by each pulse. We assume that once excited, the atom decays back to the ground state faster than the time period of the modelocked pulse train $1/R$. In this case, the atom has little memory between pulses, or equivalently, the absorption spectrum is a single broad

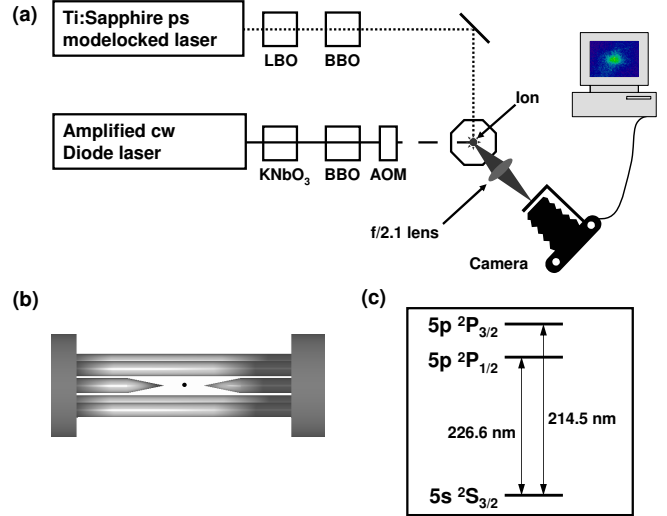


FIG. 1: The experimental apparatus. (a) Frequency-quadrupled pulses from a picosecond modelocked Ti:Sapphire laser (Spectra-Physics Tsunami) are tuned to the $5p\ ^2P_{1/2}$ transition in Cd^+ near 226.5 nm and directed onto the trapped ion. An amplified narrow-band diode laser is also frequency-quadrupled and tuned a few linewidths red of the $5P\ ^2P_{3/2}$ transition for initial Doppler cooling of the ion. An acousto-optic modulator (AOM) is used to switch on and off the narrow-band light. Photons emitted from the ion are collected by an $f/2.1$ imaging lens and directed toward a photon-counting intensified camera. (b) Schematic drawing of the linear rf trap used in the experiment, with the ion position indicated by the black dot in the middle. (c) The relevant energy levels of Cd^+ .

line of width $\Delta \sim 1/\tau$ (τ is the pulse duration) and the frequency comb of spacing R has very little contrast.

The equilibrium temperature for broadband pulsed laser cooling of trapped atoms is expected to scale approximately with the laser bandwidth Δ , and is much higher than typical narrowband laser-cooled atom temperatures. Still, cooling of atoms in a strong trap to these higher temperatures can localize them to less than the diffraction limit ($\sim 1\mu\text{m}$) of typical imaging optics. This cooling may thus be sufficient for the implementation of quantum optics applications that interface atoms

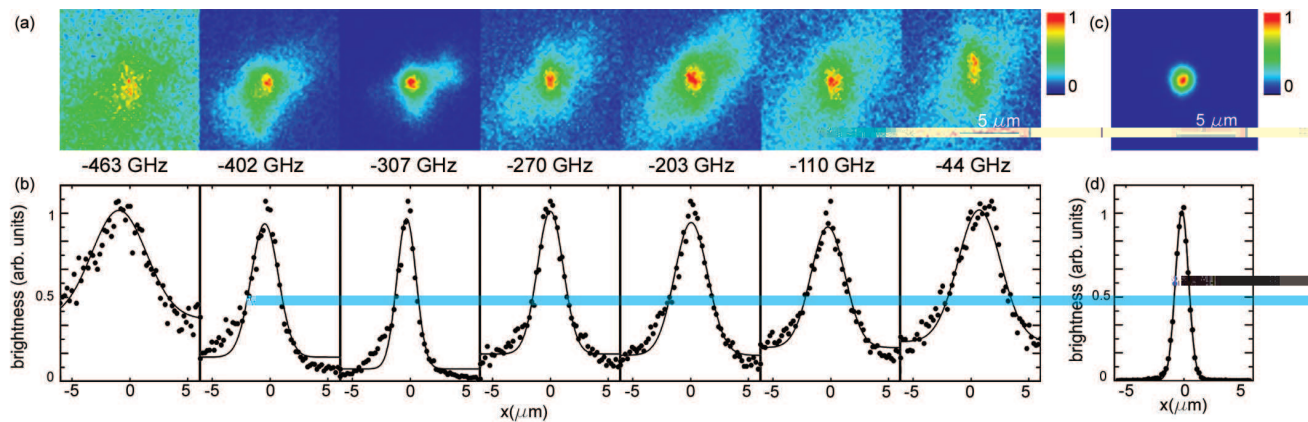


FIG. 2: (a) Images of a single trapped ion taken at various pulsed laser detunings $\delta/2\pi$ indicated at the bottom. The pulsed laser beam direction in each image is diagonal from lower-left corner to upper-right corner. (b) Crosssections of the images in (a) along the vertical direction. The solid lines are Gaussian fits to the data. (c) An image of a narrow-band laser-cooled ion localized to ~ 30 nm, with its crosssection and a Gaussian fit plotted in (d).

with photons [11, 12, 13]. In these applications, it is necessary to mode-match single photons emitted by individual atoms, so the atomic image quality is important, while cooling to near the ground state of motion or within the Lamb-Dicke limit is not required [14].

The experimental setup is shown schematically in Fig. 1. We trap atomic cadmium ions in a linear rf (Paul) trap [15], shown in Fig. 1(b). The spacing of four 0.5 mm diameter rods is about 1 mm, while the separation of the two end cap needles is about 2.6 mm. The strengths of the radial rf trap and the axial static trap are adjusted to be approximately (but not exactly) equal: $\omega_x \simeq \omega_y \simeq \omega_z \simeq 2\pi \times 0.85$ MHz, and the rf drive frequency is $\Omega_{\text{rf}} = 2\pi \times 35.8$ MHz. The trapped ions can be either Doppler-cooled with a narrow-band, cw laser tuned a few linewidths red of the $^2S_{1/2} - ^2P_{3/2}$ transition at 214.5 nm, or by a modelocked laser tuned red of the $^2S_{1/2} - ^2P_{1/2}$ transition at 226.5 nm. Both laser beams are oriented to have significant k -vector components along each principal axis of the trap to efficiently cool all degrees of freedom of the trapped ion. The ion fluorescence is collected by an f/2.1 lens and directed to a photon-counting intensified camera. The inherent chromatic aberration of the imaging system allows us to selectively image the 226.5 nm or the 214.5 nm fluorescence by simply adjusting the focus on the f/2.1 lens.

To measure the cooling efficiency of the modelocked laser we first Doppler-cool a single Cd^+ ion using the narrow-band laser, with the pulsed laser also directed onto the ion. The narrow-band laser beam is then turned off, and an image of the trapped ion fluorescence is recorded using the camera, with an integration time of up to 10 minutes. A series of broadband laser-cooled ion images taken at various detunings $\delta = \omega_l - \omega_a$, where ω_l is the modelocked laser central frequency, and ω_a is the atomic resonance frequency, is shown in Fig. 2(a).

The modelocked laser average power is held constant at 1 mW, which corresponds to individual pulse energies of about 12.5 pJ. The resulting image is analyzed to measure its rms width, x_{im} , by fitting its crosssection to a Gaussian distribution [Fig.2(b)].

To determine the actual Gaussian rms radius x_{rms} of the time-averaged ion position, two effects must be considered. First is the finite resolution x_r of the imaging optics, which we measure by recording an image of a narrowband laser-cooled ion [Fig.2(c)], resulting in a near point-source with an estimated object size of ~ 30 nm. Fitting its crosssection [Fig.2(d)] to a Gaussian distribution provides a good estimate of $x_r = 1.15 \pm 0.01 \mu\text{m}$. This is about a factor of two larger than the expected diffraction-limited image size of about $0.55 \mu\text{m}$, which we attribute to an incomplete correction of the spherical aberration of the f/2.1 lens. Using properties of the convolution of Gaussian functions, we then determine the resolution-corrected image width: $x_{\text{corr}} = \sqrt{x_{\text{im}}^2 - x_r^2}$.

The second effect is the modulation of the ion brightness due to laser light intensity variation across the waist, whose measured rms width is $x_w = 3.35 \pm 0.15 \mu\text{m}$. The true rms ion motion size is $x_{\text{rms}} = x_w x_{\text{corr}} / \sqrt{x_w^2 - x_{\text{im}}^2 \sin^2(\phi)}$, where ϕ is the angle between the laser beam direction and the direction of ion image crosssection. We analyze the temperature in the radial and the axial directions, where $\phi = \pm 45^\circ$.

The effect of the ion micromotion (fast oscillations near the rf drive frequency) on the image size is negligible in our case. With the proper compensation of the background electric fields, the micromotion amplitude is $x_m = (\sqrt{2}\omega/\Omega_{\text{rf}})x_{\text{rms}} \simeq 0.035x_{\text{rms}}$ [16], where ω is the ion's secular frequency along the particular principal axis. Broadening of the image due to excess micromotion, which arises from an incomplete compensation of the background electric fields, is taken to be much

smaller than the resolution x_r of our optics.

The ion rms velocity in the trap v_{rms} along a principal axis is directly proportional to the rms displacement: $v_{\text{rms}} = \omega x_{\text{rms}}$. The temperature T of the ion (assuming a normal distribution of its velocity) is then given by $k_B T = m v_{\text{rms}}^2$, where k_B is the Boltzmann constant, and m is the ion mass.

The summary of our results is shown in Fig. 3. For the ion temperature data in Fig. 3(a), each point is measured using the procedure described above [17]. The absorption lineshape in Fig. 3(b) is taken in a separate experiment by measuring the fluorescence rate of a single cold ion under a pulsed laser average power of 1 mW. For this, a 100 μs narrowband laser-cooling cycle is interlaced with a 200 μs period when only the pulsed laser light is incident on the ion and the ion fluorescence is collected. There is a wide range of pulsed laser detunings in Fig. 3(a) for which the ion temperature is well below 5 K, reaching as low as 1 K. These detunings correspond to the region of high slope in the absorption line curve, as expected in Doppler cooling [18]. The ion temperature increases sharply as δ approaches zero; it also grows significantly on the far-red side of the resonance, where the cooling rate is very slow due to low photon scatter rate, while additional background heating [19, 20] presumably increases the equilibrium temperature of the ion.

The bandwidth of the laser pulses used in the experiment is measured to be $\Delta \sim 2\pi \times 420$ GHz, as shown in Fig 3(b), which is almost three orders of magnitude larger than the linewidth $\gamma/2\pi \simeq 50.5$ MHz of the $5p^2P_{1/2}$ Cd^+ excited state [15]. Thus, the velocity-dependent (frictional) force that leads to cooling arises from the laser line shape rather than the atomic line shape.

The cooling mechanism can still be understood in terms similar to conventional Doppler cooling [18]. The probability of absorbing a photon by the ion is velocity-dependent, due to Doppler shifts. With the laser central frequency tuned to the red of the atomic resonance ($\delta < 0$), the atom has higher probability of absorbing a photon when it is moving towards the laser beam, experiencing a blue Doppler shift. This absorption reduces the atom velocity in the direction of motion. The following spontaneous emission is random and equally likely in any direction; thus, the net effect of absorption and emission is to lower the kinetic energy of the atom. For a bound atom, as in the case of an ion in an rf trap, only one cooling laser beam is necessary, provided that its k -vector has components along all three trap principal axes [21, 22]. The expressions derived for cooling rate and the cooling limit remain the same for a free atom and three pairs of counter-propagating cooling laser beams.

The average force due to scattering of photons from the laser beam experienced by the atom along a principal axis in the trap in this configuration is:

$$F = \Delta p R P_{\text{exc}}, \quad (1)$$

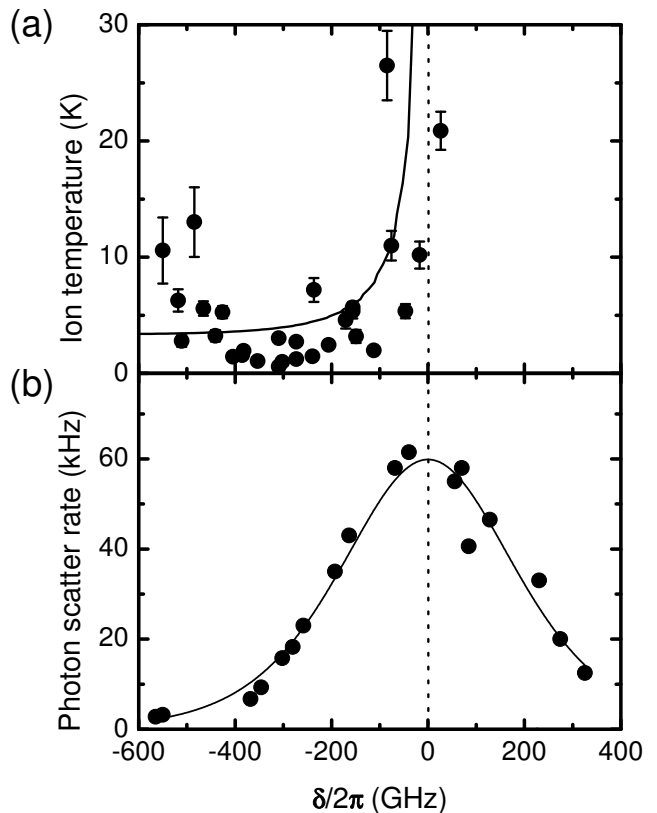


FIG. 3: A summary of the measurements. (a) The measured radial ion temperature is plotted against the pulsed laser detuning δ . The solid line represents the theoretically predicted temperature [Eq. 5]. (b) Photon scatter rate from a single, cold ion is plotted against the pulsed laser detuning. The vertical dashed line indicates the atomic resonance position, corresponding to the wavelength 226.57 nm. The solid line is a fit to the data using sech^2 spectrum [Eq. 2], indicating $\Delta \sim 420$ GHz and $\tau \simeq 1.3$ ps

where $\Delta p = \hbar k / \sqrt{3}$ is the average momentum kick along the principal axis from each photon absorption, with k being the photon's wavenumber, R the modelocked laser repetition rate, and we assume that \vec{k} has equal components along each trap axis [22]. The atomic excitation probability P_{exc} can be derived analytically for hyperbolic secant pulses $E_0 \text{sech}(\pi t / \tau)$ [23] of electric field amplitude E_0 and duration τ , expected from the modelocked laser:

$$P_{\text{exc}} = \sin^2(\theta/2) \text{sech}^2(\tau(\delta + kv)/2), \quad (2)$$

where θ is the Rabi rotation angle from a resonant laser pulse, τ is the pulse duration, and v is the atom velocity component along the laser beam.

For small values of v , the force [Eq. 1] becomes

$$F \simeq F_0 + \beta v, \quad (3)$$

where the offset force $F_0 = \Delta p R \sin^2(\theta/2) \text{sech}^2(\tau\delta/2)$

shifts the equilibrium position of the trapped atom by $F_0/(m\omega^2) \sim 1$ nm in our trap [22], and $\beta v = \Delta p k \tau R \sin^2(\theta/2) \text{sech}^2(\tau\delta/2) \tanh(\tau\delta/2) v$ is a damping force for $\delta < 0$, corresponding to red detuning of the laser, with the cooling rate β/m . In our experiment, the maximum cooling rate $\beta/m \simeq 2 \text{ sec}^{-1}$.

This cooling is opposed by diffusion heating resulting from photons emitted by the atom in random directions:

$$D = \frac{1}{3}(2E_r)RP_{\text{exc}}, \quad (4)$$

where $E_r = \frac{(\hbar k)^2}{2m}$ is the photon recoil energy, and the factor of $1/3$ is due to the diffusion energy equally distributed between the three degrees of freedom [22]. Equating the cooling power βv^2 to the heating power D , we can find the equilibrium temperature of the atom:

$$T = \frac{\hbar}{\sqrt{3}\tau k_B} \frac{1}{\tanh(\tau\delta/2)}, \quad (5)$$

where substitutions for β and P_{exc} have been made.

The predicted ion temperature T corresponding to Eq. 5 is plotted in Fig. 3(a) in a solid line. Note that this line is not a fit to the data; rather, it is a theoretical prediction based on the laser and trap parameters used in the experiment. The theory and experiment are in a good agreement for the radial measurements, while the measured axial temperatures (not shown in Fig. 3) were consistently lower than the theory [17].

It is important to point out that the lifetime of the $\text{Cd}^+ 5p^2 P_{1/2}$ excited state is only 3.146 ns [15], while the period of the laser pulses is 12.5 ns. Thus, by the time the next laser pulse arrives, the excited state population is only about 2%. This cooling process is then primarily due to absorbing single photons from individual pulses, and not due to an optical frequency comb effect [9, 10, 24]. For optimal cooling of a given atomic species, the pulsed laser repetition rate should be of the order of the atom's excited state linewidth, while the energy in each laser pulse should correspond to $P_{\text{exc}} \simeq 1$

In summary, we have observed and quantified laser-cooling of a single, trapped atom by broadband, modelocked laser pulses. The cooling is efficient, while the lowest temperatures are in single digits Kelvin. Lower temperatures should be possible if longer modelocked laser pulses are used, as predicted by Eq. 5, where the final atom temperature scales approximately as the inverse of the pulse duration τ . Such cooling of ions in strong rf traps localizes them to under $1 \mu\text{m}$, which allows diffraction-limited ion imaging.

This work was supported by the U.S. National Security Agency and Advanced Research and Development Activity under Army Research Office contract DAAD19-01-1-

0667 and the National Science Foundation Information Technology Research Program.

* Electronic address: bblinov@umich.edu

- [1] T. Hansch and A. Schawlow, *Opt. Comm.* **13**, 68 (1975).
- [2] D. J. Wineland and H. Dehmelt, *Bull. Am. Phys. Soc.* **20**, 657 (1975).
- [3] J. Hoffnalge, *Opt. Lett.* **13**, 102 (1988).
- [4] M. Zhu, C. W. Oates, and J. L. Hall, *Phys. Rev. Lett.* **67**, 46 (1991).
- [5] I. C. M. Littler, H. M. Keller, U. Gaubatz, and K. Bergmann, *Z. Phys. D.* **18**, 307 (1991).
- [6] W. Ketterle, A. Martin, M. A. Joffe, and D. E. Pritchard, *Phys. Rev. Lett.* **69**, 2483 (1992).
- [7] R. Calabrese, V. Guidi, P. Lenisa, E. Mariotti, and L. Moi, *Opt. Commun.* **123**, 530 (1996).
- [8] S. N. Atutov, R. Calabrese, R. Grimm, V. Guidi, I. Lauer, P. Lenisa, V. Luger, E. Mariotti, L. Moi, A. Peters, et al., *Phys. Rev. Lett.* **80**, 2129 (1998).
- [9] P. Strohmeier, A. Horn, T. Kersebom, and J. Schmand, *Z. Phys. D* **21**, 215 (1991).
- [10] M. Watanabe, R. Omukai, U. Tanaka, K. Hayasaka, H. Imajo, and S. Urabe, *J. Opt. Soc. Am. B* **13**, 2377 (1996).
- [11] C. Simon and W. T. M. Irvine, *Phys. Rev. Lett.* **91**, 110405 (2003).
- [12] L.-M. Duan, B. B. Blinov, D. L. Moehring, and C. Monroe, *Quantum Inf. Comput.* **4**, 165 (2004).
- [13] L.-M. Duan and R. Raussendorf, *arXiv:quant-ph/0502120* (2005).
- [14] D. Leibfried, R. Blatt, C. Monroe, and D. Wineland, *Rev. Mod. Phys.* **75**, 281 (2003).
- [15] D. L. Moehring, B. B. Blinov, D. W. Gidley, R. N. Kohn, Jr., M. J. Madsen, T. D. Sanderson, R. S. Vallery, and C. Monroe, Submitted to PRL (2005).
- [16] D. J. Berkeland, J. D. Miller, J. C. Bergquist, W. M. Itano, and D. J. Wineland, *J. Appl. Phys.* **83**, 5025 (1998).
- [17] Here, we present the analysed temperature data for radial direction in the trap only (vertical in Fig.2(a)). In the axial direction (horizontal in Fig.2(a)), the observed temperature is about 5 times lower. This suggests that our simple theoretical model does not fully describe the cooling mechanism.
- [18] H.J. Metcalf and P. van der Straten, *Laser Cooling and Trapping* (Springer, Stony Brook, NY, 1999).
- [19] R. Blümel, C. Kappler, W. Quint, and H. Walther, *Phys. Rev. A* **40**, 808 (1989).
- [20] Q. A. Turchette, D. Kielpinski, B. E. King, D. Leibfried, D. M. Meekhof, C. J. Myatt, M. A. Rowe, C. A. Sackett, C. S. Wood, W. M. Itano, et al., *Phys. Rev. A* **61**, 063418 (2000).
- [21] D. J. Wineland and W. M. Itano, *Phys. Rev. A* **20**, 1521 (1979).
- [22] W. M. Itano and D. J. Wineland, *Phys. Rev. A* **25**, 35 (1982).
- [23] N. Rosen and C. Zener, *Phys. Rev.* **40**, 502 (1932).
- [24] D. Kielpinski, *arXiv:quant-ph/0306099* (2003).